ACS Catalysis

pubs.acs.org/acscatalysis

Research Article

Molecular Design of Supported MoO_x Catalysts with Surface TaO_x Promotion for Olefin Metathesis

Bin Zhang, Shuting Xiang, Anatoly I. Frenkel, and Israel E. Wachs*

Cite This: *ACS Catal.* 2022, 12, 3226−3237

Read Online

ACCESS | Metrics & More | Article Recommendations | Supporting Information

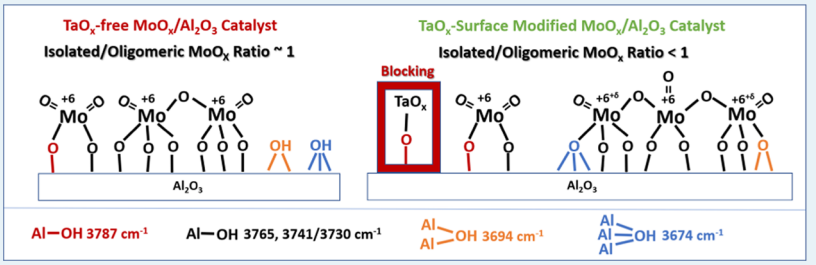

ABSTRACT: A series of supported 3% MoO_x catalysts were synthesized by incipient-wetness impregnation of a 5−15% TaO_x surface-modified γ-Al_2O_3 support. The catalysts were characterized by *in situ* spectroscopies (diffuse reflectance infrared Fourier transform spectroscopy (DRIFTS), Raman, UV−vis, X-ray absorption spectroscopy (XAS)) and multiple chemical probes (C_2H_4/C_4H_8 titration, C_3H_6-TPSR, steady-state propylene metathesis, NH_3-IR adsorption). The supported tantalum oxide phase was present as surface TaO_x sites on the γ-Al_2O_3 support that capped the Al_2O_3 surface hydroxyls. The change in available surface hydroxyls caused the subsequent anchoring of MoO_x species to occur at different surface hydroxyls. This shifted the anchoring of MoO_x species from basic (Al-OH) to neutral (Al_2-OH) to more acidic (Al_3-OH) surface hydroxyls as well as perturbation of the remaining alumina surface hydroxyls by the surface TaO_x sites. The TaO_x surface-modified γ-Al_2O_3 support increased the number of activated surface MoO_x sites (Ns) by ∼6× and the turnover frequency (TOF) by ∼10×, resulting in an increased activity of ∼60×. It was found that the specific anchoring surface hydroxyls rather than the extent of oligomerization of the surface MoO_x sites control the number of activated MoO_x sites and TOF for propylene metathesis. No relationships between the nature of the surface Lewis/Brønsted acid sites and Ns and TOF were found to be present.

KEYWORDS: *metathesis, propylene, molybdate, Raman, DRIFTS, UV−vis, XAS*

1. INTRODUCTION

Propylene is a critical chemical intermediate that is produced from the refinery, steam cracking, and on-purpose methods. The olefin metathesis reaction, as an on-purpose method for propylene production, is a reversible reaction that helps meet the global shortage of propylene. The cleavage and reformation of C=C double bonds in ethylene and 2-butene permit the production of two propylene molecules.[1−4] Industrial heterogeneous supported MoO_x/Al_2O_3 catalysts have been applied in the shell higher olefin process (SHOP) to produce linear higher olefins since 1977.[5] Although heterogeneous supported MoO_x catalysts are easily prepared, there are multiple surface MoO_x structures due to the nonuniform nature of the surfaces of oxide supports, which requires the use of advanced molecular-level characterization techniques to determine the catalytic active sites. For example, three distinct surface MoO_x structures are present on the Al_2O_3 support (isolated di-oxo MoO_4 on basic Al-OH, oligomeric $MoO_{5/6}$ on neutral Al_2-OH and acidic Al_3-OH, and crystalline MoO_3 nanoparticles).[6,7] The catalytic activity of supported MoO_x catalysts is significantly influenced by the selection of the oxide support.[8−12] The SiO_2-Al_2O_3 mixed oxide support is a highly effective support for promoting olefin metathesis in comparison to the one component Al_2O_3 or SiO_2 support. Anchoring active sites at acidic surface hydroxyls of the mixed oxide support results in a greater number of activated sites.[13] This observation motivates the current investigation to examine the influence of other mixed oxide supports, such as supported $MoO_x/TaO_x/Al_2O_3$ catalysts, for olefin metathesis. The acidity of surface Brønsted sites is often proposed to be related to improved olefin metathesis activity on mixed oxide support.[9,14] For example, Hahn et al. examined surface MoO_x sites on various oxide supports (SiO_2, Al_2O_3, SiO_2−Al_2O_3) with pyridine-IR adsorption and found that the ethylene/2-butene cross-metathesis activity increased with (i) increasing amounts

Received: December 28, 2021
Revised: February 5, 2022

https://doi.org/10.1021/acscatal.1c06000
ACS Catal. 2022, 12, 3226−3237

of Brønsted acid sites (ii) increasing oligomerization degree of the surface MoO_x sites and (iii) decreasing amounts of Lewis acid sites. It was claimed that protonation of propene to surface Mo(+4)-isopropoxide was driven by Brønsted acidic Mo-OH during activation.[9] Li et al. investigated MoO_x sites on the Hβ and γ-Al_2O_3 mixed oxide support with ^{1}H NMR and proposed that the moderate Brønsted acidity for moderate MoO_x loadings may contribute to the ethylene/2-butene cross-metathesis activity by involving into the initial MoO_x site activation.[14] Supporting data are generally lacking and the nature of the MoO_x sites and oxide support sites have not been well investigated. The absence of *in situ* investigation on well-defined model supported MoO_x catalysts has inhibited the fundamental understanding of this important catalytic reaction. To design a highly active model promoted MoO_x/Al_2O_3 catalyst, the basic alumina hydroxyls need to be selectively capped with an acidic promoter that will allow MoO_x to selectively anchor at the more acidic surface hydroxyls of the alumina support.[15]

In the present study, a TaO_x promoter was used to surface modify the Al_2O_3 support for propylene self-metathesis to ethylene and 2-butene by supported MoO_x/Al_2O_3 catalysts. The surface TaO_x promoter was selected since TaO_x is not active for olefin metathesis and gives rise to weak Raman bands that will not overshadow the Raman bands of the surface MoO_x sites.[15] The following aspects will be examined: (i) the anchoring sites of MoO_x on unpromoted and Ta-promoted Al_2O_3 support, (ii) the nature of surface MoO_x sites under dehydrated and propylene metathesis reaction conditions, and (iii) the influence of surface Lewis and Brønsted acid sites upon the activity of the propylene metathesis reaction. The objective of the present study is to establish the structure–activity relationship for olefin metathesis by supported Ta-promoted MoO_x/Al_2O_3 catalysts. The origin of the improved propylene metathesis activity on Ta-promoted MoO_x/Al_2O_3 catalysts is the consequence of modifying the MoO_x anchoring locations on the surface hydroxyls of Al_2O_3.

2. EXPERIMENTAL DETAILS

2.1. Catalyst Synthesis. The Al_2O_3 support (Sasol, Puralox, 200 m^2/g) was initially calcined at 500 °C for 16 h in flowing air to remove any combustible impurities. The Al_2O_3 support was surface-modified by incipient-wetness impregnation (IWI) of an ethanol solution of tantalum ethoxide (Ta-$(OC_2H_5)_5$, Sigma-Aldrich, 99.98%) inside a glovebox (Vacuum Atmosphere, Omni-Lab VAC 101965). After addition of TaO_x to alumina, the TaO_x/Al_2O_3 was dried overnight in a glovebox and calcined at 500 °C for 4 h. The supported 3% MoO_x catalysts were synthesized by IWI of aqueous ammonium heptamolybdate ($(NH_4)_6Mo_7O_{24}{\cdot}4H_2O$, Alfa Aesar, 99%) onto the surface TaO_x-modified Al_2O_3 support (5, 10, and 15% TaO_x). The supported 3%MoO_x/TaO_x/Al_2O_3 catalysts were dried overnight at ambient conditions, further dried at 120 °C for 2 h in flowing air, and finally calcined by ramping the temperature at 1 °C/min to 500 °C and held at 500 °C for 4 h. The surface coverage of Ta for the surface-modified TaO_x/Al_2O_3 support (5, 10, and 15% TaO_x) is 0.7, 1.4, and 2.0 Ta/nm^2 corresponding to 16, 31, and 44% monolayer surface coverage, respectively. The surface coverage of Mo for all of the supported MoO_x catalysts is 0.8 Mo/nm^2.

2.2. *In Situ* Diffuse Reflectance Infrared Fourier Transform Spectroscopy (DRIFTS). The *in situ* DRIFTS spectra of the surface-modified TaO_x/Al_2O_3 support and supported MoO_x catalysts were obtained by a Thermo Scientific Nicolet 8700 FT-IR spectrometer attached with a Harrick Praying Mantis (DRA-2). A Mercury-Cadmium-Telluride (MCT) detector was equipped to obtain the spectra with a resolution of 4 cm^{-1} with accumulations of 96 scans/min. The gas flow rates were monitored by a mass flow controller (Brooks, 5850E). Approximately, 20 mg of loose catalysts powders was loaded into an *in situ* reaction cell (Harrick, HVC–DR2 with a CaF2 window) sealed with an O-ring (Harrick, Viton). The *in situ* cell window was cooled with flowing water during the experiments. The procedure for collecting the *in situ* DRIFTS spectra was as follows: the catalyst was dehydrated at 500 °C with flowing 10% O_2/Ar (Air Gas, UHP, 30 mL/min) for 1 h. Then, the temperature was cooled to 120 °C and then flushed with Ar (Air Gas, UHP, 30 mL/min) for 30 min. The DRIFTS spectra of dehydrated catalysts were collected at 120 °C with 10% O_2/Ar. The dehydration procedure for NH_3-IR spectra was the same as indicated above. The NH_3/He (Airgas, 2000 ppm, 30 mL/min) was flowing at 120 °C for 30 min and then flushed with He (Air Gas, UHP, 30 mL/min) for 30 min. The adsorbed NH_3 was finally desorbed by ramping the temperature at 10 °C/min to 500 °C. The *in situ* DRFITS spectra were collected during the NH_3 adsorption and the temperature ramping. All of the DRIFTS spectra were normalized by the dehydrated spectra of the oxide supports.

2.3. *In Situ* Raman Spectroscopy. The *in situ* Raman spectra were obtained by a Horiba Labram HR Evolution spectrometer equipped with 4 laser sources (633, 532, 442, and 325 nm). The 442 nm laser was used for collecting *in situ* Raman spectra to minimize the sample fluorescence. The laser was focused through a confocal microscope with an X10 objective (Olympus MPLN10x). The Raman spectra were calibrated by a silicon standard possessing a reference peak at 520.7 cm^{-1}. Catalysts were loaded into an *in situ* reaction cell (Harrick Scientific HVC-MRA-5) cup padded with quartz wool, which was temperature-controlled by a Harrick ATC Temperature Controller unit. The spectra were collected with a 100 μm hole and 3 scans (20 s/scan) by a CCD camera detector (Horiba Synapse BIDD scientific), resulting in a spectral resolution of 1 cm^{-1}. Pure TiO_2 (P-25, 1%) was physically mixed with catalysts to be used as the internal standard for normalization due to the absence of Raman peaks from the pure Al_2O_3 support. The gas flow rates were monitored with the same mass flow controllers as indicated above. The procedure for collecting *in situ* Raman spectra was as follows: the catalyst was dehydrated at 500 °C in flowing 10% O_2/Ar (Air Gas, UHP, 30 mL/min) for 1 h. The temperature was then cooled to 30 °C and flushed with Ar (Air Gas, UHP, 30 mL/min) for 30 min. Subsequently, the catalysts were exposed to 5% C_3H_6/Ar (Praxair, Purity 99%, 30 mL/min) at 30 °C for 1 h and finally flushed with Ar (Air Gas, UHP, 30 mL/min) for 30 min and heated to 200 °C. The 5% C_3H_6/Ar was flowing again for 1 h and flushed with Ar at 200 °C. The *in situ* Raman spectra were collected after dehydration and during propylene metathesis at 30 and 200 °C.

2.4. *In Situ* UV–Vis Diffuse Reflectance Spectroscopy (DRS). The *in situ* UV–vis spectra of the supported MoO_x catalysts were obtained with a UV–vis-NIR spectrophotometer (Agilent Cary 5000). Approximately, 20 mg of the catalyst powder was loaded into an *in situ* reaction cell described above. The collection of each UV–vis spectrum takes ~0.6 s in the

https://doi.org/10.1021/acscatal.1c06000
ACS Catal. 2022, 12, 3226–3237

200−800 nm range. A MgO white standard was used for the reference of background absorbance. The gas flow rates were monitored with the same mass flow controllers as indicated above. The edge energy (Eg) values calculated from the UV−vis spectra were determined by the intercept of the straight line for the low-energy rise of a plot of $[F(R)h\nu]^2$ versus the incident photon energy ($h\nu$).[16] The procedure for collecting *in situ* UV−vis spectra was the same as indicated in the above *in situ* Raman experiments.

2.5. *In Situ* X-ray Absorption Spectroscopy (XAS). The *in situ* Mo K-edge X-ray absorption spectroscopy data were obtained at beamline 7-BM in the National Synchrotron Light Source-II (NSLS-II) of the Brookhaven National Laboratory (BNL). The XAS spectra were collected by ionization chamber detectors that measured transmission beam intensities through the sample and the reference (Mo) foil was used for energy calibration and alignment. Fluorescence data from the samples were measured using a PIPS detector. The catalyst pellets (~0.2 g) were loaded into an *in situ* reaction cell (Nashner−Adler).[17] A MoO_3 compound was used as the reference for comparison. The procedure for collecting the *in situ* XAS spectra was similar to that for the Raman experiments described above, but 2.5% C_3H_6/He was only flowing at 200 °C. The Athena and Artemis software programs were utilized for data processing and analysis.[18] The details of the edge X-ray absorption fine structure (EXAFS) fitting method are presented in the previous work.[13] S_0^2, the passive electron reduction factor, is fixed as 0.82 as obtained from the fitting of EXAFS data in the Mo foil.

2.6. Propylene Temperature-Programmed Surface Reaction (TPSR). The C_3H_6-TPSR spectra were obtained by an Altamira Instruments system (AMI-200). The catalysts (~0.2 g) were loaded into a U-tube quartz reactor. The dehydration procedure was similar as indicated above in Raman experiments. After flushing with Ar (Air Gas, UHP, 30 mL/min) for 30 min at 30 °C, the gas flow was switched to 5% C_3H_6/Ar (Praxair, Purity 99%, 30 mL/min) and held at 30 °C for several minutes to stabilize the MS signal. The temperature was then ramped at 10 °C/min up to 600 °C. An online Dycor ProLine Process Mass Spectrometer (MS) was employed to analyze the outgoing gases. The monitoring mass/charge channels were m/z = 18 (H_2O), m/z = 27 (C_2H_4), m/z = 42 (C_3H_6), m/z = 44 (CO_2), and m/z = 56 (C_4H_8). The MS signals were calibrated and corrected for cracking contributions from different components.

2.7. Ethylene/2-Butene Titration. The C_2H_4/C_4H_8-titration spectra were obtained by the same Altamira Instruments system (AMI-200). The initial dehydration procedure was the same as the above Raman experiments. After cooling down to 200 °C and flushing with Ar for 30 min, 2-butene was chemisorbed on the catalyst by flowing 1% C_4H_8/Ar (Praxair, Purity 99%, 30 mL/min) at 200 °C for 30 min. Afterward, the gas flow was immediately switched to 1% C_2H_4/Ar (Praxair, Purity 99%, 30 mL/min) for 30 min to titrate the adsorbed surface intermediates from 2-butene chemisorption. The same mass/charge channels were recorded as for the above C_3H_6-TPSR experiments. The number of activated surface MoO_x sites was calculated by the amount of C_3H_6 produced during $C_2H_4-C_4H_8$ titration with the assumption that only one surface Mo=$CHCH_3$ intermediate was present on the surface. The MS signals were calibrated and corrected for cracking contributions from different components.

2.8. Steady-State Propylene Metathesis. The steady-state propylene self-metathesis catalytic activity was obtained in a fix-bed reactor under differential conditions (propylene conversion <15%). Both the inlet and outlet of the gas tubes were heated to 200 °C to avoid the condensation of the propylene reactant and products (C_2H_4, C_3H_6, C_4H_8, CO_2, and H_2O) on the exit lines. Approximately, 0.2 g of the catalyst was loaded in the vertical tube reactor. The temperature was controlled by a clam shell furnace. The dehydration procedure was similar as indicated above in Raman experiments and then the reactor was cooled to 200 °C with 10% O_2/Ar and flushed with Ar (Air Gas, UHP, 30 mL/min). 1% C_3H_6/Ar (Praxair, Purity 99%, 50 mL/min) was flowing as the reactant mixture. After 1 h of reaction, the steady-state propylene metathesis conversion was obtained. An online gas chromatograph (Agilent GC 6890) equipped with a GS-Alumina (Agilent 1153552) column connected to a flame ionization detector (Agilent Model G1531) was employed to analyze the outgoing gases from the reactor. The catalytic activities (mmol/g/h) were calculated by normalizing the conversion of propylene by the flow rate and catalyst weight. The turnover frequency (TOF) values were calculated by normalizing the steady-state activity by the number of activated MoO_x sites derived from C_2H_4/C_4H_8 titration. The GC was calibrated for all of the reaction products.

3. RESULTS

3.1. *In Situ* DRIFTS of Surface Hydroxyl Anchoring Sites. The *in situ* DRIFTS spectra were collected to identify the surface hydroxyls of the Al_2O_3 support that anchor the surface TaO_x and MoO_x sites and are presented in Figure S1 and the corresponding difference spectra are presented in Figures S2 and 1. The bare Al_2O_3 support has multiple surface hydroxyls: isolated Al-OH (HO-μ_1-Al_{IV} at 3787 cm^{-1}, HO-μ_1-Al_{VI} at 3765 cm^{-1}, HO-μ_1-Al_V at 3741 and 3730 cm^{-1}), bridged Al_2-OH (HO-μ_2-Al_V at 3694 cm^{-1}), and tri-coordinated Al_3-OH (HO-μ_3-Al_{VI} at 3674 cm^{-1}).[19,20] It is well established that the (110) facet of γ-Al_2O_3 is preferentially

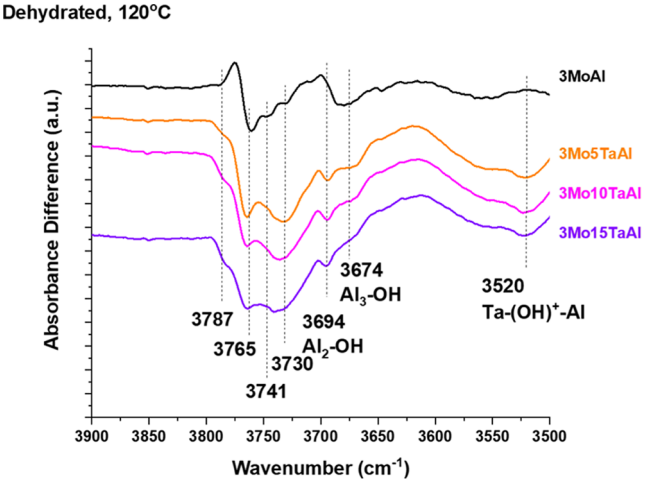

Figure 1. *In situ* DRIFTS difference spectra of the surface hydroxyl region of dehydrated supported $MoO_x/TaO_x/Al_2O_3$ catalysts (120 °C). The spectrum of the dehydrated Al_2O_3 support was subtracted from the spectrum of the 3MoAl catalyst. The spectra of dehydrated surface-modified TaO_x/Al_2O_3 supports were subtracted from the spectra of the corresponding 3MoTaAl catalysts.

https://doi.org/10.1021/acscatal.1c06000
ACS Catal. 2022, 12, 3226−3237

exposed (70−83%), while the (100) only represents a minor facet (17%).[19,21,22] The population of the γ-Al_2O_3 (111) facet is much less significant and can be neglected.[23] The HO-μ_1-Al_{IV} at 3787 cm^{-1}, HO-μ_1-Al_V at 3741/3730 cm^{-1}, and HO-μ_2-Al_V at 3694 cm^{-1} are located on the Al (110) facet, while HO-μ_1-Al_{VI} at 3765 cm^{-1} and HO-μ_3-Al_{VI} at 3674 cm^{-1} are located on the Al (100) facet.[19,20] The more basic surface hydroxyls correspond to the higher wavenumber peaks, while the lower wavenumber peaks are associated with neutral and more acidic surface hydroxyls.[24] Thus, the acidity of Al_2O_3 surface hydroxyl follows the trend: most basic Al-OH (HO-μ_1-Al_{IV}), less basic Al-OH (HO-μ_1-Al_{VI} and HO-μ_1-Al_V), neutral Al_2-OH (HO-μ_2-Al_V), and more acidic Al_3-OH (HO-μ_3-Al_{VI}). The surface hydroxyl density of Al_2O_3 is ∼6−9 OH/nm^2 with a ratio of Al_3-OH:Al_2-OH:Al-OH surface hydroxyls of ∼1.3:2:1 as determined by ^{1}H NMR.[25,26]

The surface TaO_x promoter anchors at all five types of the alumina surface hydroxyls, as indicated in Figure S2. It has been shown in prior studies that the dispersion of one metal oxide onto another metal oxide can generate new surface M_1-$(OH)^+$-M_2 Brønsted acid sites,[27,28] and thus, the newly formed peak ∼3520 cm^{-1} is assigned to the Al-$(OH)^+$-Ta Brønsted acid sites.[29] The positive peak ∼3785−3775 cm^{-1} is assigned to shifting of the basic Al-OH hydroxyl induced by the nearby surface TaO_x sites since the Ta-OH vibration is reported at lower wavenumbers (∼3680−3743 cm^{-1}).[30] Even though the preferential anchoring sites of TaO_x on Al_2O_3 are not clear from the spectra, the DRIFTS results reveal that the surface TaO_x promoter modifies the surface chemistry of the Al_2O_3 support, thereby modifying the available anchoring sites for anchoring of the MoO_x species.

For the unmodified surface MoO_x/Al_2O_3 catalyst, the surface MoO_x sites preferentially anchor at HO-μ_1-Al_{IV} (3787 cm^{-1}) and HO-μ_1-Al_{VI} (3765 cm^{-1}) surface hydroxyls. A minor amount of HO-μ_3-Al_{VI} (3674 cm^{-1}) also appears to be involved in anchoring MoO_x species. The addition of MoO_x to the surface-modified TaO_x/Al_2O_3 support shows that the MoO_x species mainly anchor at the HO-μ_1-Al_{VI} (3765 cm^{-1}), HO-μ_1-Al_V (3741/3730 cm^{-1}), HO-μ_2-Al_V (3694 cm^{-1}), HO-μ_3-Al_{VI} (3674 cm^{-1}), and the newly formed Al-$(OH)^+$-Ta (3520 cm^{-1}) Brønsted acid sites. A minor amount of HO-μ_1-Al_{IV} (3787 cm^{-1}) is also consumed by the anchoring of MoO_x. With the increase of TaO_x loading (5−15%), MoO_x sites anchor at HO-μ_1-Al_{VI} (3765 cm^{-1}), HO-μ_1-Al_V (3741/3730 cm^{-1}), and HO-μ_2-Al_V (3694 cm^{-1}). The anchoring of MoO_x at the Ta-perturbed Al-OH (3785−3775 cm^{-1}) is not significant since the peak difference is minimal after anchoring of MoO_x. In summary, compared to the unmodified supported MoO_x/Al_2O_3 catalyst, the surface MoO_x sites on the supported $MoO_x/TaO_x/Al_2O_3$ catalysts preferentially anchor at the HO-μ_1-Al_{VI} (3765 cm^{-1}), HO-μ_1-Al_V (3741/3730 cm^{-1}), HO-μ_2-Al_V (3694 cm^{-1}), and HO-μ_3-Al_{VI} (3674 cm^{-1}) surface hydroxyls.

3.2. *In Situ* Raman Spectroscopy. *3.2.1. Dehydrated Catalysts.* The *in situ* Raman spectra of the surface-modified TaO_x/Al_2O_3 support and supported MoO_x catalysts under dehydrated conditions are presented in Figures S3, S4, and 2. The γ-Al_2O_3 support does not give rise to any Raman bands.[16] For the surface-modified TaO_x/Al_2O_3 support, two main Raman bands are present at 860 and 945 cm^{-1} corresponding to the ν_s(Ta-O-Al) and ν_s(Ta═O) stretches of the surface TaO_x sites, respectively. The presence of oligomeric surface TaO_x sites is indicated by Raman bands at 617 and 715 cm^{-1}

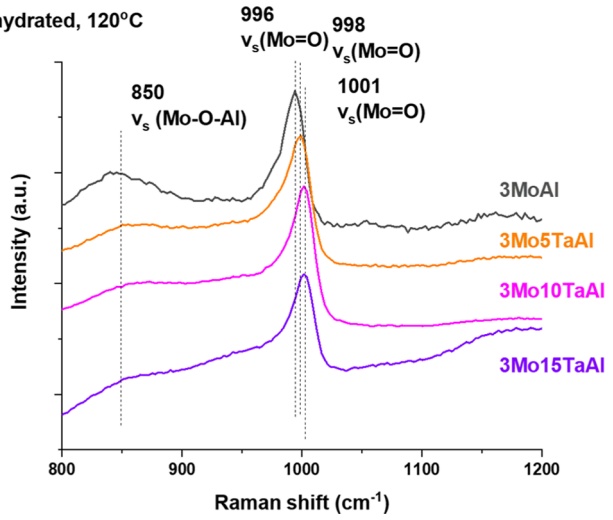

Figure 2. *In situ* Raman spectra of dehydrated supported MoO_x catalysts (120 °C, 800−1200 cm^{-1}).

corresponding to ν_s(Ta-O-Ta) and ν_{as}(Ta-O-Ta), respectively. The Raman bands at 270 and 340 cm^{-1} are characteristic of δ(Ta-O-Ta) and δ(O-Ta-O) bending modes.[31,32] For the supported $MoO_x/TaO_x/Al_2O_3$ catalysts, the Raman bands from surface TaO_x sites are too weak to be detected and the Raman spectra are dominated by the molybdenum oxide component. The absence of strong and sharp Raman bands at 820 and 960 cm^{-1} demonstrates that crystalline MoO_3 nanoparticles are not present in these catalysts. The strong Raman band at 996−1001 cm^{-1} corresponds to the ν_s(Mo═O) stretch of the surface MoO_x sites. The unpromoted 3MoAl catalysts exhibit the ν_s(Mo═O) at ∼996 cm^{-1} associated with isolated surface MoO_x sites anchored at the basic Al-OH surface hydroxyls.[6,16] The blue shift of ν_s(Mo═O) from 996 to 1001 cm^{-1} with TaO_x surface modification reflects increasing oligomerization of surface MoO_x sites with increasing surface TaO_x coverage. The blue shift is also observed in the *in situ* DRIFTS Mo═O overtone region (Figure S5). All of the supported MoO_x catalysts also exhibit a band at 850 cm^{-1} from the bridging ν_s(Mo−O−Al) vibration.

3.2.2. Propylene Metathesis Reaction Conditions. The *in situ* Raman spectra of the supported MoO_x catalysts at 60 min of propylene metathesis at 30 and 200 °C are presented in Figure 3. The spectra indicate that for the supported 3MoAl catalyst, the intensity of the ν_s(Mo═O) band is minimally perturbed at both 30 and 200 °C. In contrast, the ν_s(M═O) band of the supported 3Mo15TaAl catalyst is only minimally perturbed at 30 °C, but there is a moderate decrease in intensity at 200 °C. This observation reflects the ability of propylene to activate the surface MoO_x sites present on the TaO_x surface-modified alumina support.

3.3. UV−Vis DRS Spectroscopy. *3.3.1. Dehydrated Conditions.* The *in situ* UV−vis spectra and edge energy (Eg) values of dehydrated supported MoO_x/Al_2O_3 catalysts at 120 °C are presented in Figure 4 and Table 1. The surface TaO_x sites on Al_2O_3 exhibit UV−vis edge energy values of ∼5.0−4.6 eV that reflect the extensive oligomerization of the surface TaO_x sites with increasing surface TaO_x coverage. To remove the contribution of the surface TaO_x sites at ∼230−245 nm from the UV−vis spectra (Figure S6), the UV−vis spectra of the corresponding Mo-free TaO_x/Al_2O_3 supports were subtracted from the corresponding spectra. The resulting

https://doi.org/10.1021/acscatal.1c06000
ACS Catal. 2022, 12, 3226−3237

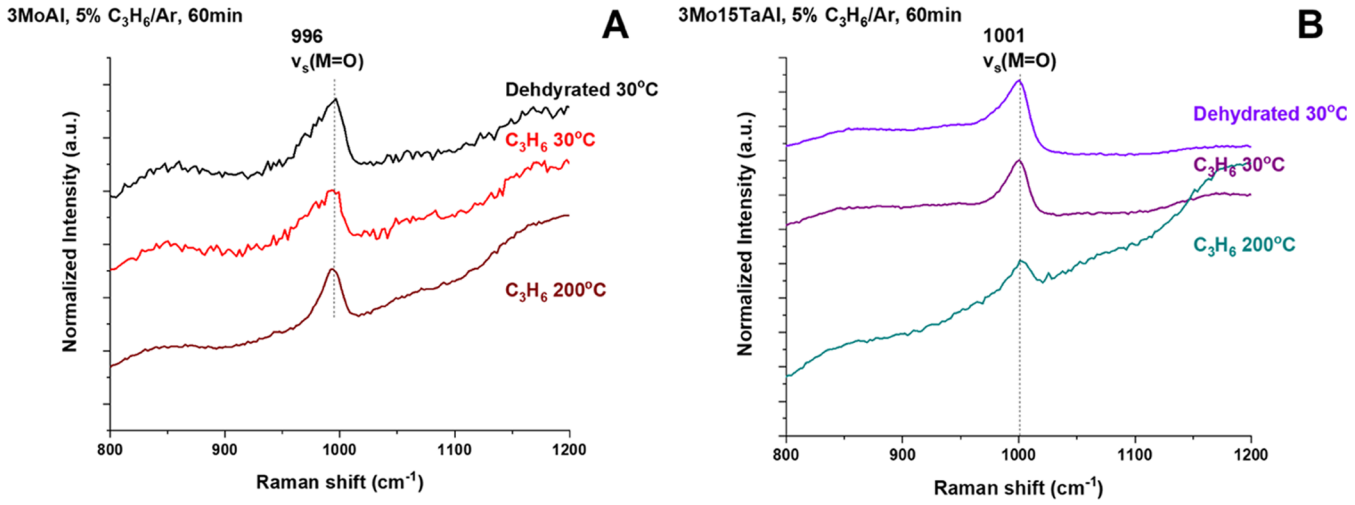

Figure 3. *In situ* Raman spectra of supported MoO_x catalysts under dehydrated conditions and at 60 min of propylene metathesis: (A) 3MoAl, (B) 3Mo15TaAl.

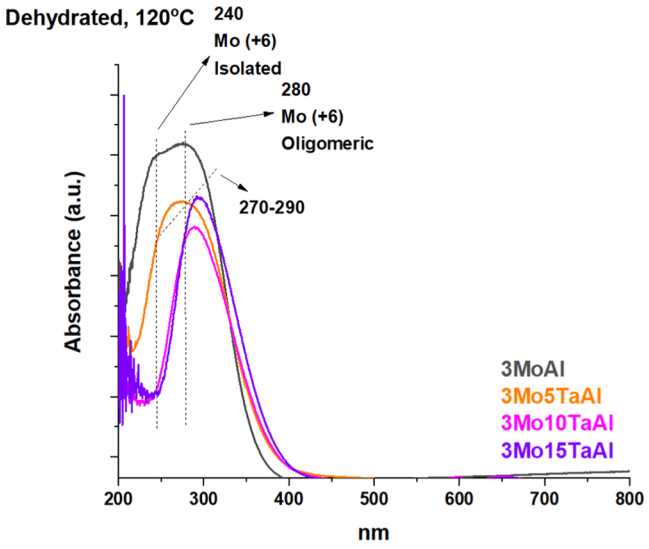

Figure 4. *In situ* UV−vis DRS spectra of dehydrated supported MoO_x/Al_2O_3 catalysts (120 °C). The UV−vis DRS spectra of dehydrated supported 3MoTaAl catalysts are generated by subtracting the contribution of the corresponding dehydrated supported TaO_x/Al_2O_3 catalysts.

Table 1. *In Situ* UV−Vis Edge Energy Values of Dehydrated Supported MoO_x Catalysts (120 °C)

catalysts	3MoAl	3Mo5TaAl	3Mo10TaAl	3Mo15TaAl
UV−vis edge energy (dehydrated)	3.9 eV	3.8 eV	3.8 eV	3.8 eV

UV−vis edge energy reflects the degree of oligomerization of the surface MoO_x sites, which are minimally affected by the presence of the surface TaO_x sites. The $MgMoO_4$ reference compound consists of isolated MoO_4 sites and exhibits a high UV−vis edge energy of ∼4.5 eV with a single ligand-to-metal charge transfer (LMCT) peak at 250 nm.[6,16,33] The $(NH_4)_2Mo_2O_7$ reference compound contains MoO_x chains with a UV−vis edge energy (Eg) value of ∼3.5 eV and two LMCT peaks at 250 and 320 nm reflecting the oligomeric structure.[6,16,33] The supported 3MoAl catalyst has an intermediate edge energy value of ∼3.9 eV with two comparable intensity LMCT peaks at 240 and 285 nm, suggesting that isolated surface MoO_x sites co-exist with oligomeric surface MoO_x sites (Figure S7). The supported 3MoTaAl catalysts have a slightly lower edge energy ∼3.8 eV with an increase in the ratio of the 285/240 nm LMCT peaks with increasing surface TaO_x coverage reflects the presence of greater amounts of oligomeric surface MoO_x sites (Figure S7). The UV−vis LMCT peaks at ∼240 and 270−290 nm of the dehydrated supported MoO_x catalysts indicate that the surface MoO_x sites are fully oxidized as Mo(+6) under dehydrated conditions.[16] This is further confirmed by the absence of UV−vis d−d peaks at ∼350−800 nm from reduced surface MoO_x sites. Thus, the surface MoO_x sites are present in the Mo^{6+} oxidation state and consist of both isolated and oligomeric sites, with the extent of oligomerization increasing with surface TaO_x coverage.

3.3.2. Propylene Metathesis Reaction Conditions. The *in situ* UV−vis difference spectra of the supported MoO_x catalysts under propylene metathesis reaction conditions at 30 and 200 °C are presented in Figure 5. The LMCT peaks at 245−280 nm from the fully oxidized Mo(+6) are minimally perturbed at 30 °C and the absence of peaks in the d−d region from reduced Mo sites. This suggests that the surface MoO_x sites on both the supported 3MoAl and 3Mo15TaAl catalysts possess surface Mo(+6) sites at 30 °C. Only when the reaction temperature is raised to 200 °C, the supported 3Mo15TaAl catalyst exhibits a very weak and broad peak (only visible in difference spectra) at ∼435 nm in the d−d region with the LMCT peaks of fully oxidized Mo(+6) minimally perturbed. The possible presence of some reduced surface Mo sites, however, could not be determined since adsorbed olefins also give rise to UV−vis peaks in the same region.[34−36] In summary, the isolated and oligomeric surface MoO_x sites appear to be minimally perturbed by the propylene metathesis reaction conditions.

3.4. *In Situ* X-ray Absorption Spectroscopy (XAS). The *in situ* X-ray absorption near edge structure (XANES) and extended X-ray absorption fine structure (EXAFS) spectra at the Mo K-edge of the supported MoO_x/Al_2O_3 and supported $MoO_x/TaO_x/Al_2O_3$ catalysts under dehydrated conditions and propylene metathesis reaction conditions are presented in Figures 6 and S8. The EXAFS fitting results are presented in

https://doi.org/10.1021/acscatal.1c06000
ACS Catal. 2022, 12, 3226−3237

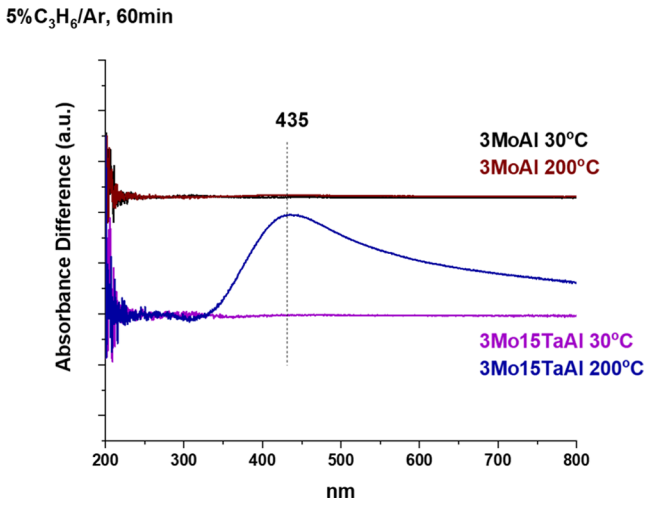

Figure 5. *In situ* UV−vis difference spectra of the supported MoO_x catalysts during propylene metathesis reaction conditions (30 and 200 °C). The spectra of the dehydrated supported MoO_x catalysts were subtracted from the spectra of the corresponding supported MoO_x catalysts under propylene metathesis reaction conditions.

Tables S1−S2 and Figures S9−S10. The MoO_4 coordination without inversion symmetry has a strong pre-edge peak due to the 1s(Mo) → 4d(Mo) + 2p(O) transition, but this transition is suppressed for the regular MoO_6 coordination with inversion symmetry.[37] A weak pre-edge peak due to this transition for MoO_6 coordination is present, however, for the distorted MoO_6 coordination (MoO_3 reference compound). Thus, the relatively strong pre-edge peak of all of the supported MoO_x catalysts at 20 003 eV is consistent with the presence of MoO_4 surface sites. The XANES edge jump (maximum of the first derivative) of all of the supported MoO_x catalysts at ∼20 015 eV is in the same position as that of the $Mo^{6+}O_3$ reference compound, indicating the oxidation state of surface MoO_x sites to be Mo(+6).[37] The k^2-weighted Mo K-edge EXAFS spectra demonstrate a strong peak at 1.2 Å (not corrected for photoelectron phase shift) corresponding to the terminal Mo═O bond that is shorter than the Mo−O bond at 1.6 Å in the MoO_2 reference compound with regular MoO_6 coordination[38] in the first shell (1−2 Å) of the Mo center. There is no Mo−Mo interaction in the second shell (3−4 Å) of the surface Mo center. The same Mo═O peak position suggests that the Mo═O bond lengths are the same for all the supported MoO_x catalysts. The surface MoO_x sites are minimally perturbed (Figure S8) during the propylene metathesis reaction at 200 °C for all of the supported MoO_x catalysts. Given that oxygen and carbon atoms have close atomic masses, the difference between Mo−O and Mo−C interactions cannot be captured by EXAFS. Quantitative model fitting of EXAFS yields a Mo═O bond at ∼1.74 Å (Tables S1 and S2). The model fitted coordination number (CN) of the Ta-promoted MoO_x/Al_2O_3 catalyst increases slightly from 3.9(4) to 4.3(4) as the concentration of TaO_x increases from 0 to 15%, reflecting the increasing amount of oligomerized surface $MoO_{5/6}$ sites on the Ta-promoted catalysts.

3.5. Chemically Probing Surface Acid Sites with NH_3-IR. The *in situ* DRIFTS spectra of Al_2O_3, TaO_x/Al_2O_3, supported 3%MoO_x/Al_2O_3, and supported 3%$MoO_x/TaO_x/Al_2O_3$ catalysts after NH_3 chemisorption are presented in Figure 7. All of the spectra exhibit the presence of surface Lewis acid sites ($\delta_{as}(NH_3{*})$ and $\delta_s(NH_3{*})$ at ∼1619 and 1252 cm^{-1}, respectively) and Brønsted acid sites ($\delta_{as}(NH_4^+{*})$ and $\delta_s(NH_4^+{*})$ at ∼1447−1480 and 1684−1697 cm^{-1}, respectively).[32,39] The initial bare Al_2O_3 support exhibits the presence of both surface Lewis and Brønsted acid sites. The Brønsted acidity of the Al_2O_3 support is relatively weak since Brønsted acidity is not detected when chemically probed by the pyridine weaker base.[24,32,39] The IR $\delta_{as}(NH_4^+{*})$ and $\delta_s(NH_3{*})$ vibrations will be used for comparison of acidity strength since they are much stronger bands. The essentially same peak position of $\delta_s(NH_3{*})$ indicates that the acid strength of the surface Lewis acid sites is similar for all of the catalysts. The vibrations from the surface Lewis acid sites are predominantly associated with the Al_2O_3 and TaO_x/Al_2O_3 supports since the surface MoO_x coverage is relatively low (0.8 Mo/nm^2) compared to the surface TaO_x coverage (0.7, 1.4,

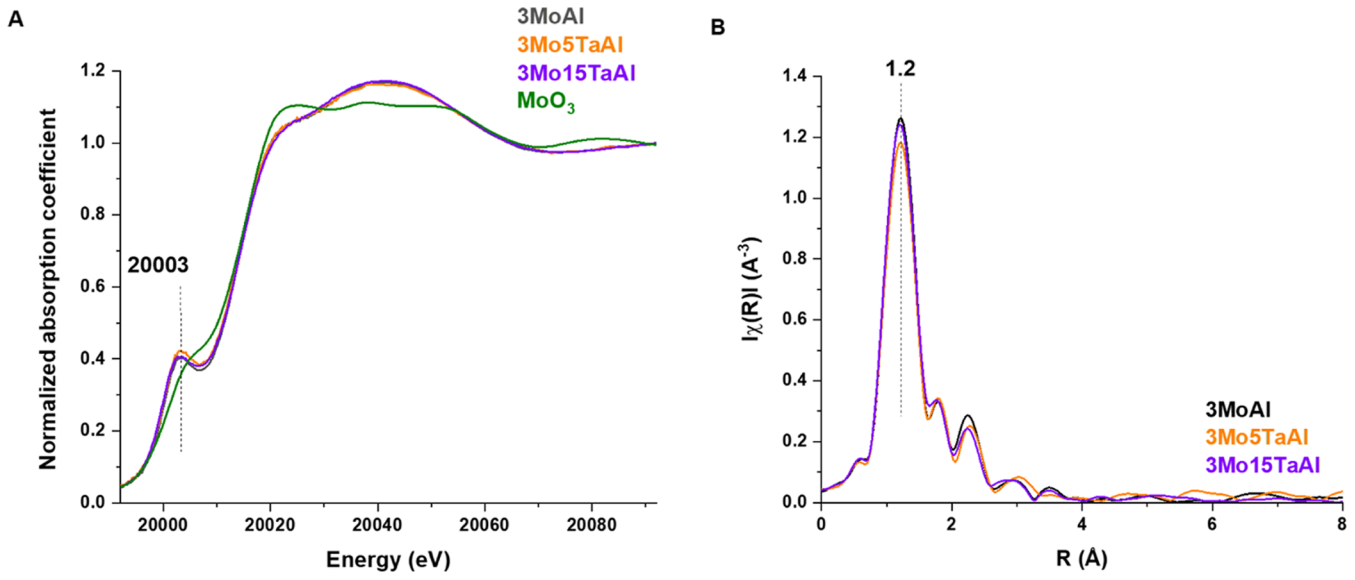

Figure 6. (A) Mo K-edge XANES spectra of dehydrated catalysts. (B) Fourier transform (FT) magnitude of the k^2-weighted Mo K-edge EXAFS data of catalysts (200 °C). The *k*-range for FT was from 2 to 10 $Å^{-1}$.

https://doi.org/10.1021/acscatal.1c06000
ACS Catal. 2022, 12, 3226−3237

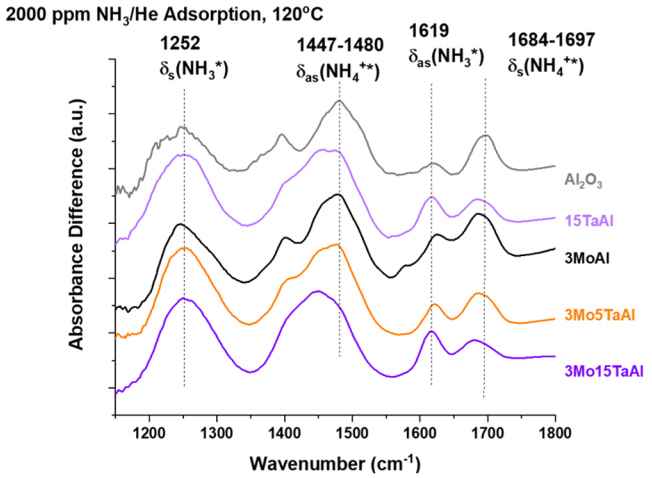

Figure 7. *In situ* DRIFTS spectra of dehydrated supported MoO_x catalysts after NH_3 adsorption and evacuation at 120 °C.

2.0 Ta/nm^2). The addition of both surface MoO_x sites and the TaO_x surface modifier introduces weaker Brønsted acid sites, as indicated by the red shift of $\delta_{as}(NH_4^+*)$ peak. With increasing surface TaO_x coverage, the Brønsted acidity of the supported 3MoTaAl catalysts is dominated by the weaker surface TaO_x Brønsted acid sites. The Brønsted acidity strength introduced by MoO_x is in-between that of Al_2O_3 and surface TaO_x sites as indicated by the moderate red shift of $\delta_{as}(NH_4^+*)$. The strength of surface Brønsted acidity follows the trend Al_2O_3 > 3MoAl > 15TaAl ~ 3Mo5TaAl > 3Mo15TaAl. Since DRIFTS is not quantitative, only the relative ratios of the Brønsted/Lewis acid sites can be compared: Al_2O_3 (1.54) > 3MoAl (1.46) > 3Mo5TaAl (1.32) > 15TaAl (1.29) > 3Mo15TaAl (1.21). The peak areas of the Brønsted acid sites follow the trend: 15TaAl (16.7) > 3Mo5TaAl (16.3) > 3Mo15TaAl (15.7) ~ 3MoAl (15.6) ≫ Al_2O_3(12.7). In summary, all of the catalysts have surface Lewis acid sites with similar strength, while the addition of the surface MoO_x and TaO_x sites introduces weaker surface Brønsted acid sites.

3.6. Propylene-TPSR. The C_3H_6-TPSR spectra of the supported MoO_x catalysts are presented in Figure 8. The supported 3MoAl catalyst produces C_4H_8 from 30 to 600 °C with a peak temperature (Tp) of ~480−500 °C. The supported 3MoTaAl catalysts, however, form C_4H_8 in several temperature ranges: ~50−150 °C (Tp = 65 °C), ~225−375 °C (Tp = 280−310 °C), and ~375−600 °C (Tp = 480−510 °C). The C_3H_6-TPSR spectra suggest that there are probably 3 distinct active surface MoO_x sites in these catalysts with their specific activity increasing with the decreasing Tp value. Both the amount of C_4H_8 produced and specific activity tend to increase with increasing surface TaO_x coverage reflecting the promotional effect of the surface TaO_x sites upon propylene metathesis by the supported $MoO_x/TaO_x/Al_2O_3$ catalysts.

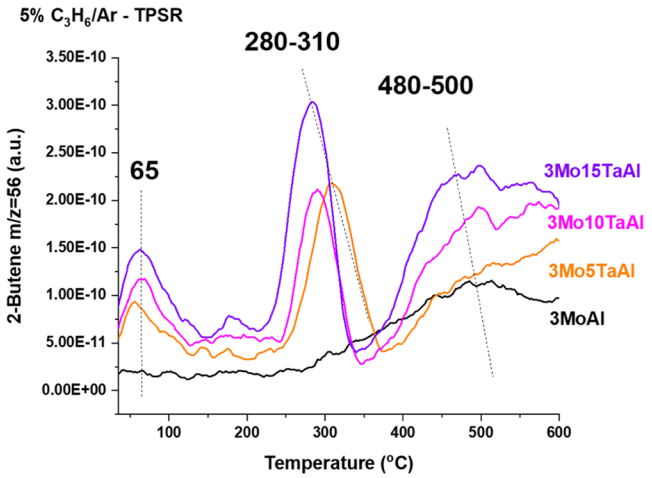

Figure 8. Propylene-TPSR spectra for the supported 3%MoO_x/n% TaO_x/Al_2O_3 catalysts from 30 to 600 °C (n = 0, 5, 10, 15).

3.7. Ethylene/2-Butene Titration (Number of Active Sites). The number of catalytic active sites involved in olefin metathesis can be determined from the number of propylene molecules formed during ethylene/2-butene titration.[40,41] The time-resolved titration spectra are presented in Figure 9. The propylene produced during the ethylene/2-butene titration shows that the surface intermediate Mo=$CHCH_3$ becomes titrated by ethylene within the first 10 min after switching from 2-butene to ethylene. The Mo-free Al_2O_3 and TaO_x/Al_2O_3 supports do not yield any propylene from the C_2H_4/C_4H_8 titration, which indicates that the catalytic active site for olefin metathesis is the surface MoO_x sites. The fraction of activated surface MoO_x sites from the $C_2^=/C_4^=$ titration is given in Table 2. The supported 3MoAl possesses a small fraction of activated surface MoO_x sites (~3.2%) with the addition of surface TaO_x sites increasing the fraction of activated surface MoO_x sites by ~5−6× (~16−19%). Thus, the number of activated surface MoO_x sites is significantly increased by surface modification of the Al_2O_3 support with surface TaO_x sites.

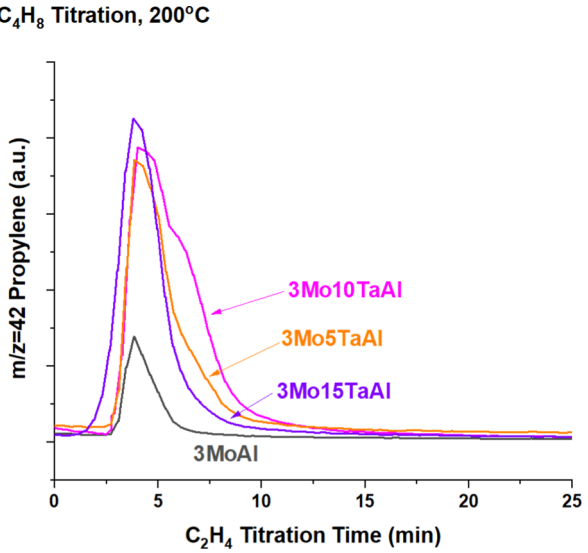

Figure 9. Time-resolved MS spectra of C_3H_6 produced during the titration of surface Mo=$CHCH_3$ with C_2H_4 for the supported MoO_x catalysts (200 °C).

3.8. Steady-State Propylene Metathesis. The steady-state catalytic activities of the supported MoO_x catalysts for propylene self-metathesis at 200 °C are presented in Table 2. The activity trend is 3Mo15TaAl > 3Mo10TaAl > 3Mo5TaAl ≫ 3MoAl. The turnover frequency (TOF) values were calculated by dividing the catalytic activity by the number of activated surface MoO_x sites determined from C_2H_4/C_4H_8 titration and are presented in Table 2. The TOF value increases approximately one order of magnitude with the

https://doi.org/10.1021/acscatal.1c06000
ACS Catal. 2022, 12, 3226−3237

Table 2. Fraction of Activated Surface MoO_x Sites Calculated from C_2H_4/C_4H_8 Titration, Steady-State Activity, and Propylene Metathesis Turnover Frequency (TOF)

	3MoAl	3Mo5TaAl	3Mo10TaAl	3Mo15TaAl
fraction of activated surface MoO_x sites	3.2%	16.3%	18.8%	18.1%
steady-state activity (mmol/g/h)	0.0056	0.2274	0.2986	0.3466
TOF (s^{-1})	2.4×10^{-4}	1.9×10^{-3}	2.1×10^{-3}	2.6×10^{-3}

addition of surface TaO_x sites to the Al_2O_3 support. Thus, the TOF value for surface MoO_x sites is significantly promoted by surface modification of the Al_2O_3 support with surface TaO_x sites.

4. DISCUSSION

4.1. Surface Anchoring Hydroxyls for MoO_x Sites. The surface hydroxyls of the Al_2O_3 and TaO_x/Al_2O_3 supports serve as the anchoring sites for the deposition of the TaO_x and MoO_x species (Figure 1). The MoO_x species for the supported 3MoAl catalyst preferentially anchor at the most basic Al-OH (HO-μ_1-Al_{IV}) and less basic Al-OH (HO-μ_1-Al_{VI}) surface hydroxyls with a minor amount also anchoring at the less basic Al-OH (HO-μ_1-Al_V) and acidic Al_3-OH surface hydroxyls. The anchoring of the surface TaO_x species on Al_2O_3, however, indiscriminately involves all five types of the surface hydroxyls and form new Brønsted acid Al-$(OH)^+$-Ta sites. Consequently, the anchoring of the surface TaO_x species affects the remaining surface hydroxyls available for the subsequent anchoring of the MoO_x species. The surface TaO_x sites partly cap the most basic Al-OH (HO-μ_1-Al_{IV}) surface hydroxyls, thus, shifting the anchoring of MoO_x to the less basic Al-OH (HO-μ_1-Al_{VI} and HO-μ_1-Al_V), neutral Al_2-OH, and acidic Al_3-OH surface hydroxyls usually observed with the anchoring of MoO_x at intermediate surface coverage.[6]

For the supported $ReO_x/TaO_x/Al_2O_3$ catalyst system, TaO_x surface modification of Al_2O_3 was previously found to shift the anchoring of ReO_x species from the most basic Al-OH (HO-μ_1-Al_{IV}) to the neutral Al_2-OH and acidic Al_3-OH surface hydroxyls.[15] Although the trend with surface TaO_x modification is similar for both the supported $ReO_x/TaO_x/Al_2O_3$ and $MoO_x/TaO_x/Al_2O_3$ catalyst systems (less anchoring at the most basic surface hydroxyls and anchoring at less basic, neutral, and acidic surface hydroxyls), the specific anchoring sites of ReO_x and MoO_x are not exactly the same probably because of the different acidity of the MoO_x and ReO_x species.

4.2. Molecular Structure of Dehydrated Surface MoO_x Sites. The dehydrated supported 3MoAl catalyst contains both isolated surface MoO_4 sites (LMCT peak at ~240 nm (Figure S7), higher UV−vis Eg value (Table 1), and lower EXAFS coordination number (Table S1)) and oligomeric $MoO_{5/6}$ sites (LMCT peak at ~285 nm (Figure S7), intermediate UV−vis Eg value (Table 1), and higher EXAFS coordination number (Table S1)). The dehydrated supported 3MoTaAl catalysts also contain isolated MoO_4 and oligomeric $MoO_{5/6}$ sites with the fraction of oligomeric $MoO_{5/6}$ sites increasing with surface TaO_x coverage (increase in the UV−vis peak at ~285 nm relative to ~240 nm (Figure S7), blue shift of the ν_s(Mo═O) band position (Figure 2), and higher EXAFS coordination number (Table S1)). For all of the supported MoO_x catalysts, the oxidation state of MoO_x sites is predominantly Mo(+6) (absence of d−d peaks and XANES edge jump). The change of the molecular structure of the surface MoO_x sites on the supported 3MoTaAl catalysts is a consequence of the modification of the available anchoring surface hydroxyls on the Al_2O_3 support brought about by TaO_x surface modification.

The molecular structure of the surface MoO_x sites supported on Al_2O_3 has been extensively studied with *in situ* Raman,[6,7,16,42] XAS,[7,42,43] *in situ* UV−vis,[6,16] and density functional theory (DFT).[23,44−46] Three distinct surface MoO_x sites are present on Al_2O_3 that depend on the surface MoO_x coverage. At low surface coverage (<1 Mo/nm^2), the surface is dominated by isolated di-oxo MoO_4 sites. At high surface coverage (1−4.6 Mo/nm^2), both isolated di-oxo MoO_4 sites and oligomeric mono-oxo $MoO_{5/6}$ surface sites co-exist. Above monolayer coverage (>4.6 Mo/nm^2), crystalline MoO_3 nanoparticles form on top of the surface MoO_x monolayer.[6,7,16,42,43] The molecular structure of the surface MoO_x sites for the supported 3MoAl catalyst reported herein agrees with structures of the surface MoO_x sites on MoO_x/Al_2O_3 at low MoO_x surface coverage previously reported in the literature. The molecular structures of the surface MoO_x sites for the supported 3MoTaAl catalysts, however, correspond to the structures present at intermediate surface MoO_x coverage of the supported 9−13% MoO_x/Al_2O_3 catalysts (Figure 2 and Table 1). The number of terminal oxo Mo═O bonds depends on the specific support: di-oxo and mono-oxo MoO_x sites co-exist on Al_2O_3,[6] ZrO_2,[16,47] and TiO_2[48] and di-oxo MoO_x sites on SiO_2.[16,33,49] Since the MoO_x species mainly anchor at the Al_2O_3 surface hydroxyls of TaO_x surface-modified Al_2O_3, both di-oxo and mono-oxo surface MoO_x sites most likely co-exist for the supported 3MoTaAl catalysts. Only when one of the anchoring sites for the MoO_x species is selectively capped by the surface TaO_x site, the number of terminal Mo═O bonds in the remaining surface MoO_x site can be clearly determined with isotopic $^{18}O-^{16}O$ exchange.[15] Two distinct surface ReO_4 sites were identified on supported ReO_4/Al_2O_3 catalysts. The surface TaO_x sites completely block the formation of the surface ReO_4-I sites at basic hydroxyls and shift anchoring of the surface ReO_4 species to more neutral and acidic surface hydroxyls.[15] The observed molecular structural change of the surface MoO_x sites for the supported 3MoTaAl catalyst suggests that surface TaO_x on Al_2O_3 similarly blocks anchoring of MoO_x species at basic surface hydroxyls (Figures 1, S1, and S2). The blocking effect of the surface TaO_x sites for the supported MoO_x/Al_2O_3 catalysts, however, is weaker than that for the corresponding supported ReO_x/Al_2O_3 catalysts, where all of the isolated surface ReO_4 sites at low coverage become blocked since not all of the isolated surface MoO_4 sites are blocked by the surface TaO_x sites. Consequently, isolated surface MoO_4 sites are still present for the supported $MoO_x/TaO_x/Al_2O_3$ catalyst.

4.3. Molecular Structure of Surface MoO_x Sites during Propylene Metathesis. To perform propylene metathesis, the surface MoO_x sites require activation by propylene, resulting in the removal and replacement of terminal Mo═O bonds by surface molybdenum carbenes (Mo═CH_3 and Mo═$CHCH_3$).[50] The molecular structures of the surface MoO_x sites of the supported 3MoAl catalyst are not perturbed during propylene metathesis at 30 and 200 °C (minimal changes in Raman (Figure 3), UV−vis (Figure 5),

https://doi.org/10.1021/acscatal.1c06000
ACS Catal. 2022, 12, 3226−3237

and XAS (Figure S8 and Tables S1, S2)). In contrast, the surface MoO_x sites for the supported 3MoTaAl catalysts are modestly activated under propylene metathesis reaction at 200 °C (Figure 3, decrease in Raman intensity from propylene coordination). The oxidation state of the surface MoO_x sites for both 3MoAl and 3MoTaAl catalysts under propylene metathesis reaction remains dominated by Mo(+6) (minimal perturbation of the UV−vis LMCT peak (Figures 4 and 5) and XANES edge jump (Figures 6 and S8)) since the dehydrated surface MoO_x sites and activated molybdenum carbene both exhibit Mo(+6) (Figure 5).[5,6,8,51]

The nature of the surface MoO_x sites on Al_2O_3 during propylene metathesis has recently been examined by *in situ* Raman spectroscopies as a function of MoO_x loading.[6] For supported MoO_x/Al_2O_3 catalysts at low surface MoO_x coverage, the isolated MoO_4 sites dominate under propylene metathesis reaction conditions and do not become activated at low temperatures (<200 °C).[6] The findings in the present study for the supported 3MoAl catalyst during propylene metathesis (Figure 3) are in agreement with the previously reported findings.

The *in situ* Raman spectra of supported ReO_4/Al_2O_3 catalysts revealed that the surface ReO_4-I sites anchored at basic Al-OH surface hydroxyls are minimally activated during propylene metathesis, while the surface ReO_4-II sites anchored at neutral Al_2-OH and more acidic Al_3-OH are extensively activated at low temperatures (<200 °C). The Ta-surface-modified supported ReO_4/Al_2O_3 catalysts only contain the surface ReO_4-II sites; formation of surface ReO_4-I is not present since the basic Al-OH sites have been capped by the surface TaO_x sites and are extensively activated at low temperatures (30 °C).[15] Similar to the Ta-surface-modified supported ReO_4/Al_2O_3 catalysts, activation of the surface MoO_x sites for the Ta-surface-modified supported $MoO_x/TaO_x/Al_2O_3$ catalyst by propylene is enhanced because some of the basic Al-OH surface hydroxyls are capped by the surface TaO_x sites that increase anchoring of the MoO_x species at less basic, neutral, and more acidic surface hydroxyl sites (Figures 1, S1, and S2).

4.4. Structure−Activity Relationship for Propylene Metathesis. Typically, the fraction of activated surface metal alkylidene species is only a fraction of the total supported metal oxides.[13,40,52−60] The steady-state reaction and C_2H_4/C_4H_8 titration reveal that both the number of activated surface MoO_x sites and the TOF values increase with surface TaO_x coverage (Table 2: 3Mo15TaAl > 3Mo10TaAl > 3Mo5TaAl ≫ 3MoAl). A similar trend is also found for activation (C_3H_6-TPSR) of the supported MoO_x catalysts at low, intermediate, and high temperatures (Figure 8: 3Mo15TaAl > 3Mo10TaAl > 3Mo5TaAl ≫ 3MoAl). These trends correspond to two changes (i) anchoring surface hydroxyls for the surface MoO_x sites and (ii) extent of oligomerization of the surface MoO_x sites. Given that both variables are varying at the same time, it appears at first difficult to determine the contributions of these variables to activation and TOF. However, the analogous supported $ReO_4/TaO_x/Al_2O_3$ catalysts only contain isolated surface ReO_4 sites and the surface TaO_x changes the anchoring surface hydroxyls of the surface ReO_4 sites. Given that both olefin metathesis catalyst systems behave similarly with surface metal oxide coverage and surface TaO_x modification, it appears that the dominant factor is the anchoring sites and not the oligomerization extent of the surface MoO_x sites.

DFT calculations of activated surface Mo-methylidene sites found that the location of the surface MoO_x sites on the Al_2O_3 support influences the activity of the surface Mo-methylidene toward ethylene addition.[23,44−46,61] The calculations predicted that on the (100) and (110) facets of Al_2O_3, when Mo-methylidene was anchored at neutral Al_2-OH or more acidic Al_3-OH surface hydroxyls, the surface MoO_x sites were less stable with a decreased electron density of the molybdenum center, making the geometry of the surface Mo-methylidene more suitable for olefin addition.[23,46] Both monomeric and dimeric MoO_x sites can become activated sites, but the latter requires a lower activation energy. Dimeric surface MoO_x sites are more stable on the Al (100) facet, while isolated MoO_x sites are more stable on the Al (110) facet.[44,45] These studies indicate that the isolated surface Mo-methylidene is less active since such sites prefer to form the less active square-pyramidal molybdacyclobutane surface intermediate. Thus, the DFT calculations also indicate the importance of surface anchoring sites for activation of surface MoO_x sites for olefin metathesis.

For Ta-free supported MoO_x/Al_2O_3 catalysts, the amount of C_4H_8 formation during C_3H_6-TPSR at high temperatures remains constant with surface MoO_x coverage.[6] On the Ta-surface-modified MoO_x/Al_2O_3 catalysts, however, the amount of C_4H_8 production at high temperatures increases with surface TaO_x coverage (Figure 8). This difference is ascribed to the modification of the basic Al-OH surface hydroxyls by the surface TaO_x sites involved in anchoring isolated surface MoO_4 sites (Figures 1, S1, and S2). Analogously, the increase in production of C_4H_8 at intermediate and low temperatures is related to the perturbation of the surface hydroxyls by the surface TaO_x sites involved in anchoring the MoO_x species at less basic Al-OH ($HO\text{-}\mu_1\text{-}Al_V$) and neutral Al_2-OH of Al(110) and less basic Al-OH ($HO\text{-}\mu_1\text{-}Al_{VI}$) and acidic Al_3-OH of Al(100), respectively. Thus, the activation and specific catalytic activity of surface MoO_x sites on the Al_2O_3 support can be tuned by modification of the available surface hydroxyl anchoring sites.

4.5. Influence of Surface Lewis/Brønsted Acidity on Propylene Metathesis. In the present study, the dehydrated supported MoO_x catalysts were found to possess very similar strength of Lewis acid sites (dominated by Lewis acid sites of the Al_2O_3 and TaO_x/Al_2O_3 supports) and slightly weaker Brønsted acid sites (Figure 7). A relationship between Lewis acidity and propylene metathesis activity could not be established since the Lewis acidity is dominated by the oxide supports at the low surface MoO_x coverage (0.8 Mo/nm^2 that corresponds to ∼18% of the monolayer) employed in the present study. There is no relationship between Brønsted acid strength and propylene metathesis activity since the addition of surface TaO_x sites decreases the strength of the Brønsted acid sites, while the propylene metathesis activity increases. The amount of Brønsted acid sites also does not relate with propylene metathesis activity since both the supported 3MoAl and 3Mo15TaAl catalysts have comparable amounts of Brønsted acid sites and the supported 3Mo15TaAl catalyst is much more active for propylene metathesis.

The surface acidity properties of surface TaO_x and MoO_x sites on Al_2O_3 have been documented in several studies.[24,62−64] Adsorption of pyridine on the Mo-free supported TaO_x/Al_2O_3 indicated that (i) at low surface TaO_x coverage, only weak Lewis acid sites are present and the amount of Lewis acid sites increase with TaO_x loading, and (ii) at high surface TaO_x coverage, the amount of Brønsted acid sites increase and

https://doi.org/10.1021/acscatal.1c06000
ACS Catal. 2022, 12, 3226−3237

the strength of the Lewis acid sites decrease with increasing TaO_x loading.[62] For supported MoO_x/Al_2O_3 catalysts, NH_3-TPD reveals that the total amount of acid sites initially increases and then decreases with increasing surface MoO_x coverage.[65] Pyridine-IR adsorption on supported MoO_x/Al_2O_3 catalysts indicates that the amount of Brønsted acid sites linearly increases with the addition of surface MoO_x sites. The trend of the amount of Lewis acid sites with surface MoO_x coverage, however, is still under debate. Boorman et al. and Turek et al. found the amount of Lewis acid sites increase with MoO_x addition, while Segawa et al. found the opposite trend.[24,63,64] The different surface acidity trends proposed from literatures may be related to the use of different Al_2O_3 support materials. Recent DFT calculations proposed that the surface silanol of SiO_2 interact with surface MoO_x sites constituting Brønsted acid sites that could play a key role in activating the surface active sites.[66] To minimize the influence of the oxide support contribution, pyridine-IR adsorption studies need to be performed since ammonia is too strong a basic probing molecule. Attempts have also been made to determine possible correlations between propylene metathesis activity and surface Lewis/Brønsted acidity of supported MoO_x catalysts. Hahn et al. and Li et al. proposed a correlation between Brønsted acidity and ethylene/2-butene cross-metathesis activity as addressed in the Introduction section.[9,14] Uchagawkar et al. examined supported MoO_x/Silicate(TUD-1) catalysts with pyridine-IR adsorption and found that the amount of surface Lewis acid sites linearly correlated to the ethylene/2-butene cross-metathesis activity.[10] Otroshchenko et al. investigated supported MoO_x catalysts on individual (ZrO_2, TiO_2, Al_2O_3, SiO_2) and mixed oxide supports (ZrO_2−SiO_2, ZrO_2−PO_4, TiO_2−SiO_2; Al_2O_3−SiO_2) with pyridine-IR adsorption and NH_3-TPD. No general relationships between olefin metathesis activity and strength/amount of Lewis/Brønsted sites could be established.[12] A general conclusion about the influence of surface acid sites on olefin metathesis cannot be made from the above literature findings since these studies are clearly not consistent with each other. Possible reasons for these different observations are the use of oxide supports from different sources and the presence of surface impurities. The present detailed study, however, finds that there are no relationships between surface Lewis or Brønsted acid sites and olefin metathesis.

5. CONCLUSIONS

A series of novel TaO_x−surface-modified supported MoO_x/Al_2O_3 catalysts for propylene metathesis were successfully synthesized and well-characterized. The TaO_x surface modifier perturbs the surface hydroxyl chemistry of the Al_2O_3 support, which alters the available surface hydroxyls for subsequent anchoring of the MoO_x species. Consequently, the surface MoO_x species anchor at basic Al-OH surface hydroxyls perturbed by TaO_x, more neutral Al_2-OH, and acidic Al_3-OH surface hydroxyls that facilitate activation and propylene metathesis activity of the resulting surface MoO_x sites. The resulting catalytic properties are dependent on the anchoring surface hydroxyls and not on the extent of oligomerization of the surface MoO_x sites and surface Lewis/Brønsted acidity. This study demonstrates for the first time that olefin metathesis activity, number of active sites (Ns), and TOF for supported MoO_x catalysts can be tuned by modifying the nature of the anchoring surface hydroxyls on the Al_2O_3 support.

ASSOCIATED CONTENT

Supporting Information

The Supporting Information is available free of charge at https://pubs.acs.org/doi/10.1021/acscatal.1c06000.

DRIFTS spectra (3500−3900 cm^{-1}); DRIFTS difference spectra (3500−3900 cm^{-1}); Raman spectra (TaO_x/Al_2O_3); Raman spectra (200−1200 cm^{-1}); DRIFTS spectra (1800−2150 cm^{-1}); UV−vis spectra (TaO_x/Al_2O_3); UV−vis spectra deconvolution; XANES/EXAFS spectra after reaction; EXAFS fitting (k space) under dehydration and after reaction; EXAFS fitting (R space) under dehydration and after reaction (PDF)

AUTHOR INFORMATION

Corresponding Author

Israel E. Wachs − *Operando Molecular Spectroscopy and Catalysis Laboratory, Department of Chemical & Biomolecular Engineering, Lehigh University, Bethlehem, Pennsylvania 18015, United States;* orcid.org/0000-0001-5282-128X; Email: iew0@lehigh.edu

Authors

Bin Zhang − *Operando Molecular Spectroscopy and Catalysis Laboratory, Department of Chemical & Biomolecular Engineering, Lehigh University, Bethlehem, Pennsylvania 18015, United States;* orcid.org/0000-0003-4940-8800

Shuting Xiang − *Department of Materials Science and Chemical Engineering, Stony Brook University, Stony Brook, New York 11794, United States; Division of Chemistry, Brookhaven National Laboratory, Upton, New York 11973, United States*

Anatoly I. Frenkel − *Department of Materials Science and Chemical Engineering, Stony Brook University, Stony Brook, New York 11794, United States; Division of Chemistry, Brookhaven National Laboratory, Upton, New York 11973, United States;* orcid.org/0000-0002-5451-1207

Complete contact information is available at: https://pubs.acs.org/10.1021/acscatal.1c06000

Notes

The authors declare no competing financial interest.

ACKNOWLEDGMENTS

This work was supported by the U.S. Department of Energy, Office of Science, Office of Basic Energy, Catalysis Science Program, under Award Number FG02-93ER14350. XAS analysis by AIF was supported by the National Science Foundation under Grant No. CHE-1903576. This research used beamline 7-BM (QAS) of the National Synchrotron Light Source-II, a U.S. DOE Office of Science User Facility operated for the DOE Office of Science by the Brookhaven National Laboratory (BNL) under Contract No. DE-SC0012704. The QAS beamline operations were supported in part by the Synchrotron Catalysis Consortium (U.S. DOE, Office of Basic Energy Sciences, grant number DE-SC0012335). The authors would like to acknowledge Steven Ehrlich, Nebojsa Marinkovic, and Lu Ma of 7-BM for their technical assistance.

REFERENCES

(1) Trnka, T. M.; Grubbs, R. H. The Development of L2X2Ru=CHR Olefin Metathesis Catalysts: An Organometallic Success Story. *Acc. Chem. Res.* **2001**, *34*, 18−29.

(2) Schrock, R. R. High Oxidation State Multiple Metal−Carbon Bonds. *Chem. Rev.* **2002**, *102*, 145−180.

(3) Schrock, R. R.; Hoveyda, A. H. Angew. Molybdenum and Tungsten Imido Alkylidene Complexes as Efficient Olefin-Metathesis Catalysts. *Angew. Chem., Int. Ed.* **2003**, *42*, 4592−4633.

(4) Grubbs, R. H. *Handbook of Metathesis*; Wiley-VCH: Weinheim, 2015, pp 1−32.

(5) Mol, J. C. Industrial applications of olefin metathesis. *J. Mol. Catal. A: Chem.* **2004**, *213*, 39−45.

(6) Chakrabarti, A.; Wachs, I. E. Molecular Structure−Reactivity Relationships for Olefin Metathesis by Al2O3-Supported Surface MoOx Sites. *ACS Catal.* **2018**, *8*, 949−959.

(7) Hu, H.; Wachs, I. E.; Bare, S. R. Surface Structures of Supported Molybdenum Oxide Catalysts: Characterization by Raman and Mo L3-Edge XANES. *J. Phys. Chem. A* **1995**, *99*, 10897−10910.

(8) Lwin, S.; Wachs, I. E. Olefin Metathesis by Supported Metal Oxide Catalysts. *ACS Catal.* **2014**, *4*, 2505.

(9) Hahn, T.; Bentrup, U.; Armbruster, M.; Kondratenko, E. V.; Linke, D. The Enhancing Effect of Brønsted Acidity of Supported MoOx Species on their Activity and Selectivity in Ethylene/trans-2-Butene Metathesis. *ChemCatChem* **2014**, *6*, 1664−1672.

(10) Uchagawkar, A.; Ramanathan, A.; Hu, Y.; Subramaniam, B. Highly dispersed molybdenum containing mesoporous silicate (Mo-TUD-1) for olefin metathesis. *Catal. Today.* **2020**, *343*, 215−225.

(11) Handzlik, J.; Ogonowski, J.; Stoch, J.; Mikolajczyk, M. Comparison of metathesis activity of catalysts prepared by anchoring of MoO2(acac)2 on various supports. *Catal Lett.* **2005**, *101*, 65−69.

(12) Otroshchenko, T.; Zhang, Q.; Kondratenko, E. Room-Temperature Metathesis of Ethylene with 2-Butene to Propene Over MoOx-Based Catalysts: Mixed Oxides as Perspective Support Materials. *Catal. Lett.* **2021**, DOI: 10.1007/s10562-021-03822-2.

(13) Zhang, B.; Lwin, S.; Xiang, S.; Frenkel, A. I.; Wachs, I. E. Tuning the Number of Active Sites and Turnover Frequencies by Surface Modification of Supported ReO4/(SiO2−Al2O3) Catalysts for Olefin Metathesis. *ACS Catal.* **2021**, *11*, 2412−2421.

(14) Li, X.; Zhang, W.; Liu, S.; Xu, L.; Han, X.; Bao, X. Olefin Metathesis over Heterogeneous Catalysts: Interfacial Interaction between Mo Species and a Hβ-Al2O3 Composite Support. *J. Phys. Chem. C* **2008**, *112*, 5955−5960.

(15) Lwin, S.; Keturakis, C.; Handzlik, J.; Sautet, P.; Li, Y.; Frenkel, A. I.; Wachs, I. E. Surface ReOx Sites on Al2O3 and Their Molecular Structure−Reactivity Relationships for Olefin Metathesis. *ACS Catal.* **2015**, *5*, 1432−1444.

(16) Tian, H.; Roberts, C. A.; Wachs, I. E. Molecular Structural Determination of Molybdena in Different Environments: Aqueous Solutions, Bulk Mixed Oxides, and Supported MoO3 Catalysts. *J. Phys. Chem. C* **2010**, *114*, 14110−14120.

(17) Nashner, M. S.; Frenkel, A. I.; Adler, D. L.; Shapley, J. R.; Nuzzo, R. G. Structural Characterization of Carbon-Supported Platinum−Ruthenium Nanoparticles from the Molecular Cluster Precursor PtRu5C(CO)16. *J. Am. Chem. Soc.* **1997**, *119*, 7760−7771.

(18) Ravel, B.; Newville, M. ATHENA, ARTEMIS, HEPHAESTUS: data analysis for X-ray absorption spectroscopy using IFEFFIT. *J. Synchrotron Radiat.* **2005**, *12*, 537−541.

(19) Digne, M.; Sautet, P.; Raybaud, P.; Euzen, P.; Toulhoat, H. Hydroxyl Groups on yAlumina Surfaces: A DFT Study. *J. Catal.* **2002**, *211*, 1−5.

(20) Digne, M.; Sautet, P.; Raybaud, P.; Euzen, P.; Toulhoat, H. Use of DFT to achieve a rational understanding of acid-basic properties of γ-alumina surfaces. *J. Catal.* **2004**, *226*, 54−68.

(21) Knözinger, H.; Ratnasamy, P. Catalytic Aluminas: Surface Models and Characterization of Surface Sites. *Catal. Rev.* **1978**, *17*, 31−70.

(22) Alvarez, L. J.; Sanz, J. F.; Capitán, M. J.; Centeno, M. A.; Odriozola, J. A. Surface models for γ-Al2O3 from molecular dynamics simulations. *J. Chem. Soc., Faraday Trans.* **1993**, *89*, 3623−3628.

(23) Handzlik, J. Properties and metathesis activity of monomeric and dimeric Mo centres variously located on γ-alumina − A DFT study. *Surf. Sci.* **2007**, *601*, 2054−2065.

(24) Turek, A. M.; Wachs, I. E.; Decanio, E. Acidic Properties of Alumina-Supported Metal Oxide Catalysts: An Infrared Spectroscopy Study. *J. Phys. Chem. B* **1992**, *96*, 5000−5007.

(25) Kraus, H.; Prins, R. Proton NMR Investigations of Surface Hydroxyl Groups on Oxidic Mo−P/γ -Al2O3 Catalysts. *J. Catal.* **1996**, *164*, 260−267.

(26) Ravenelle, R. M.; Copeland, J. R.; Kim, W. G.; Crittenden, J. C.; Sievers, C. Structural Changes of γ-Al2O3-Supported Catalysts in Hot Liquid Water. *ACS. Catal.* **2011**, *1*, 552−561.

(27) Hensen, E. J. M.; Poduval, D. G.; Degirmenci, V.; Ligthart, D. A. J. M.; Chen, W.; Mauge, F.; Rigutto, M. S.; Rob van Veen, J. A. Acidity Characterization of Amorphous Silica−Alumina. *J. Phys. Chem. C* **2012**, *116*, 21416−21429.

(28) Mouat, A. R.; George, C.; Kobayashi, T.; Pruski, M.; van Duyne, R. P.; Marks, T. J.; Stair, P. C. Highly Dispersed SiOx/Al2O3 Catalysts Illuminate the Reactivity of Isolated Silanol Sites. *Angew. Chem.* **2015**, *127*, 13544−13549.

(29) Kitano, T.; Okasaki, S.; Shishido, T.; Teramura, K.; Tanaka, T. Generation of Brønsted acid sites on Al2O3-supported Ta2O5 calcined at high temperatures. *Catal. Today.* **2012**, *192*, 189−196.

(30) Ushikubo, T.; Wada, K. Vapor Phase Beckmann Rearrangement over Silica-Supported Tantalum Oxide Catalysts. *J. Catal.* **1994**, *148*, 138−148.

(31) Chen, Y.; Fierro, J. L. G.; Tanaka, T.; Wachs, I. E. Supported Tantalum Oxide Catalysts: Synthesis, Physical Characterization, and Methanol Oxidation Chemical Probe Reaction. *J. Phys. Chem. B.* **2003**, *107*, 5243−5250.

(32) Nakamoto, K. *IR and Raman Spectra of Inorganic and Coordination Compounds. Part A: Theory and Application in Inorganic Chemistry*, 6th ed.; Wiley: New Jersey, 2009; pp 173−191.

(33) Lee, E. L.; Wachs, I. E. In Situ Spectroscopic Investigation of the Molecular and Electronic Structures of SiO2 Supported Surface Metal Oxides. *J. Phys. Chem. C* **2007**, *111*, 14410−14425.

(34) Aritani, H.; Tanaka, T.; Funabiki, T.; Yoshida, S.; Eda, K.; Sotani, N.; Kudo, M.; Hasegawa, S. Study of the Local Structure of Molybdenum-Magnesium Binary Oxides by Means of Mo L3-Edge XANES and UV-Vis Spectroscopy. *J. Phys. Chem. D* **1996**, *100*, 19495−19501.

(35) Wulfers, M. J.; Jentoft, F. C. Identification of carbonaceous deposits formed on H-mordenite during alkane isomerization. *J. Catal.* **2013**, *307*, 204−213.

(36) Wulfers, M. J.; Tzolova-Müller, G.; Villegas, J. I.; Murzin, Y. D.; Jentoft, F. C. Evolution of carbonaceous deposits on H-mordenite and Pt-doped H-mordenite during n-butane conversion. *J. Catal.* **2012**, *296*, 132−142.

(37) Shiju, N. R.; Rondinone, A. J.; Mullins, D. R.; Schwartz, V.; Overbury, S. H.; Guliants, V. V. XANES Study of Hydrothermal Mo-V-Based Mixed Oxide M1-Phase Catalysts for the (Amm)oxidation of Propane. *Chem. Mater.* **2008**, *20*, 6611−6616.

(38) Ressler, T.; Timpe, O.; Neisius, T.; Find, J.; Mestl, G.; Dieterle, M.; Schlogl, R. Time-Resolved XAS Investigation of the Reduction/Oxidation of MoO3-x. *J. Catal.* **2000**, *191*, 75−85.

(39) Busca, G. The surface acidity of solid oxides and its characterization by IR spectroscopic methods. An attempt at systematization. *Phys. Chem. Chem. Phys.* **1999**, *1*, 723−736.

(40) Lwin, S.; Wachs, I. E. Determination of Number of Activated Sites Present during Olefin Metathesis by Supported ReOx/Al2O3 Catalysts. *ACS Catal.* **2015**, *5*, 6823−6827.

(41) Handzlik, J.; Ogonowski, J. Dynamic Chemical Counting of Active Centers of Molybdena−Alumina Metathesis Catalysts. *Catal. Lett.* **2003**, *88*, 119−122.

https://doi.org/10.1021/acscatal.1c06000
ACS Catal. 2022, 12, 3226−3237

(42) Chen, K.; Xie, S.; Bell, A. T.; Iglesia, E. Structure and Properties of Oxidative Dehydrogenation Catalysts Based on MoO3/Al2O3. *J. Catal.* **2001**, *198*, 232−242.
(43) Aritani, H.; Fukuda, O.; Miyaji, A.; Hesegawa, S. Structural change of molybdenum on silica-alumina in contact with propene studied by ESR and Mo LIII-edge XANES. *Appl. Surf. Sci.* **2001**, *180*, 261−269.
(44) Handzlik, J.; Sautet, P. Structure of Dimeric Molybdenum(VI) Oxide Species on γ-Alumina: A Periodic Density Functional Theory Study. *J. Phys. Chem. C* **2010**, *114*, 19406−19414.
(45) Handzlik, J.; Sautet, P. Structure of Isolated Molybdenum(VI) Oxide Species on γ-Alumina: A Periodic Density Functional Theory Study. *J. Phys. Chem. C* **2008**, *112*, 14456−14463.
(46) Handzlik, J.; Ogonowski, J.; Tokarz-Sobieraj, R. Dependence of metathesis activity of Mo-methylidene sites on their location on (100) γ-Al2O3 - a theoretical study. *Catal. Today.* **2005**, *101*, 163−173.
(47) Weckhuysen, B. M.; Jehng, J.-M.; Wachs, I. E. In Situ Raman Spectroscopy of Supported Transition Metal Oxide Catalysts: 18O2-16O2 Isotopic Labeling Studies. *J. Phys. Chem. B* **2000**, *104*, 7382−7387.
(48) Tsilomelekis, G.; Boghosian, S. In Situ Raman and FTIR Spectroscopy of Molybdenum(VI) Oxide Supported on Titania Combined with 18O/16O Exchange: Molecular Structure, Vibrational Properties, and Vibrational Isotope Effects. *J. Phys. Chem. C* **2011**, *115*, 2146−2154.
(49) Chempath, S.; Zhang, Y.; Bell, A. T. DFT Studies of the Structure and Vibrational Spectra of Isolated Molybdena Species Supported on Silica. *J. Phys. Chem. C* **2007**, *111*, 1291−1298.
(50) Imamoglu, Y.; Zumeroglu-Karan, B.; Amass, A. J. *Olefin Metathesis and Polymerization Catalysts: Synthesis, Mechanism and Utilization*; Kluwer Academic: Dordrecht, The Netherlands, 1989; Vol. *326*, pp 247−269.
(51) Grunert, W.; Stakheev, A. Y.; Morke, W.; Feldhaus, R.; Anders, K.; Shpiro, E. S.; Minachev, K. M. Reduction and metathesis activity of MoO3/Al2O3 catalysts: I. An XPS investigation of MoO3/AI2O3 catalysts. *J. Catal.* **1992**, *135*, 269−286.
(52) Zhang, B.; Wachs, I. E. Identifying the Catalytic Active Site for Propylene Metathesis by Supported ReOx Catalysts. *ACS Catal.* **2021**, *11*, 1962−1976.
(53) Chauvin, Y.; Commereuc, D. Chemical Counting and Characterization of the Active Sites in the Rhenium Oxide/Alumina Metathesis Catalyst. *J. Chem. Soc., Chem. Commun.* **1992**, 462−464.
(54) Salameh, A.; Copéret, C.; Basset, J.-M.; Böhm, V. P. W.; Röper, M. Rhenium(VII) Oxide/Aluminum Oxide: More Experimental Evidence for an Oxametallacyclobutane Intermediate and a Pseudo-Wittig Initiation Step in Olefin Metathesis. *Adv. Synth. Catal.* **2007**, *349*, 238−242.
(55) Salameh, A.; Baudouin, A.; Soulivong, D.; Boehm, V.; Roeper, M.; Basset, J.-M.; Copéret, C. CH3-ReO3 on γ-Al2O3: Activity, selectivity, active site and deactivation in olefin metathesis. *J. Catal.* **2008**, *253*, 180−190.
(56) Mahmood, C. S.; Yarmo, M. A.; Hamid, S. B. D.-A. Determination of active centres in Re2O7-Al2O3 metathesis catalysts by titration method. *J. Mol. Catal. A: Chem.* **2000**, *161*, 11−16.
(57) Kapteijn, F.; Bredt, H. L. G.; Homburg, E.; Mol, J. C. Kinetics of the Metathesis of Propene over Re2O7/γ-Al2O3. *Ind. Eng. Chem. Prod. Res. Dev.* **1981**, *20*, 457−466.
(58) Ding, K.; Gulec, A.; Johnson, A. M.; Drake, T. L.; Wu, W.; Lin, Y.; Weitz, E.; Marks, L. D.; Stair, P. C. Highly Efficient Activation, Regeneration, and Active Site Identification of Oxide-Based Olefin Metathesis Catalysts. *ACS Catal.* **2016**, *6*, 5740−5746.
(59) Amakawa, K.; Wrabetz, S.; Krohnert, J.; Tzolova-Muller, G.; Schlogl, R.; Trunschke, A. In Situ Generation of Active Sites in Olefin Metathesis. *J. Am. Chem. Soc.* **2012**, *134*, 11462−11473.
(60) Amakawa, K.; Krohnert, J.; Wrabetz, S.; Frank, B.; Hemmann, F.; Jager, C.; Schlogl, R.; Trunschke, A. Active Sites in Olefin Metathesis over SupportedMolybdena Catalysts. *ChemCatChem* **2015**, *7*, 4059−4065.
(61) Handzlik, J. Metathesis Activity and Properties of Mo−Alkylidene Sites Differently Located on Silica. A Density Functional Theory Study. *J. Phys. Chem. B* **2005**, *109*, 20794−20804.
(62) Baltes, M.; Kytokivi, A.; Weckhuysen, B. M.; Schoonheydt, R. A.; Voort, P. V. D.; Vansant, E. F. Supported Tantalum Oxide and Supported Vanadia-tantala Mixed Oxides: Structural Characterization and Surface Properties. *J. Phys. Chem. B* **2001**, *105*, 6211−6220.
(63) Boorman, P. M.; Kydd, R. A.; Sarbak, Z.; Somogyvari, A. Surface Acidity and Cumene Conversion. *J. Catal.* **1985**, *96*, 115−121.
(64) Segawa, K.; Hall, W. K. Catalysis and surface chemistry: III. The adsorption of pyridine on molybdena-alumina catalysts. *J. Catal.* **1982**, *76*, 133−143.
(65) Marakatti, V. S.; Mumbaraddi, D.; Shanbhag, G. V.; Halgeri, A.; Maradur, S. P. Molybdenum oxide/g-alumina: an efficient solid acid catalyst for the synthesis of nopol by Prins reaction. *RSC Adv.* **2015**, *5*, 93452.
(66) Handzlik, J.; Kurleto, K.; Gierada, M. Computational Insights into Active Site Formation during Alkene Metathesis over a MoOx/SiO2 Catalyst: The Role of Surface Silanols. *ACS Catal.* **2021**, *11*, 13575−13590.

https://doi.org/10.1021/acscatal.1c06000
ACS Catal. 2022, 12, 3226−3237